A. F. Diaz
K. K. Kanazawa

Electrodes with Covalently Attached Monolayers

We have used cyclic and second-harmonic ac voltammetry to study solution and solid state electrochemical reactions on metal oxide surfaces chemically modified with silyl derivatives of the type $SnO_2/Si(CH_2)_3NH(CH_2)_xNR_1R_2$. *The R groups studied include pyrazoline derivatives, tetrathiafulvalene, and ferrocene. Electrode effects on solution redox reactions involving phenothiazine and benzoquinone have also been compared using both platinum electrodes and the chemically modified electrodes. The results from the various approaches used consistently indicate that the redox reactions are slower on modified as opposed to unmodified electrode surfaces.*

Introduction

An understanding of the structure and properties of surfaces has clear application in many technological areas; electrochemistry, liquid and gas chromatography, enzyme immobilization, chemical synthesis, photocells, adhesion, lubrication, and corrosion are a few examples. Thus, there is a continuing need to develop expertise in the generation of stable surfaces with predictable chemical and physical properties.

A survey of the literature reveals that earlier studies in this area were based on surfaces containing molecules or thin films prepared by absorption or deposition methods. However, in the last three years several laboratories have approached this problem by focusing on chemically modified electrode surfaces such as TiO_2, PtO_2, RuO_2, Al_2O_3, SiO_2, doped SnO_2, and oxidized carbon [1-7]. With this approach, molecules of interest are covalently attached to metal oxide surfaces. The attractiveness of this approach is that control is now exercised over the stoichiometry and the molecular geometry of the surface molecules.

The usual procedure for surface modification involves treating the surface with aminoalkylsilyl derivatives such as 3-aminopropyltriethoxysilane or 3-(2-aminoethyl) propyltrimethoxysilane. These reagents are particularly convenient because the silyl groups react with surface oxygen to form stable covalent bonds while the amino group at the other end of the molecule is free to undergo additional reactions by means of standard synthetic procedures.

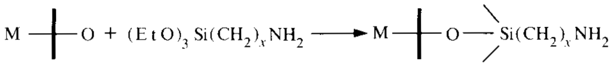

$$M-O + (EtO)_3Si(CH_2)_xNH_2 \longrightarrow M-O-Si(CH_2)_xNH_2$$

This type of surface modification is fairly new, and many questions regarding the structure and reactivity of these surface molecules must be addressed before one can effectively parameterize and design new surfaces with predictable chemical and physical properties. The intent of this presentation is to focus on those aspects of our research that provide insight into the chemical nature of these surfaces. We address three basic questions: the nature of the metal oxide-alkylsilyl bonding, the chemical stability of the surface-attached radical intermediates, and the molecular dynamics associated with the electrochemical reactions.

The molecular dynamics of surface molecules during electrochemical reactions have been probed in several situations. The experiments were designed to provide information about 1) how the aminoalkylsilyl derivative influences the electron-transfer process between the electrode and the electroactive structure when it is attached to the amino group; 2) how the aminoalkylsilyl derivative influences radical dimer formation when the radicals are attached to the amino group; and 3) how the electroinactive aminoalkylsilyl monolayer influences electron transfer between the electrode and a dissolved electroactive species.

Monolayer structure

Characterization of a modified Sn-O surface by examination with x-ray photoelectron spectroscopy (ESCA) has provided useful information regarding the nature of these surfaces. It is known that the organic film has Sn-O-Si surface ether bonds, is 0.1-0.14 nm (10-14 Å) thick, is primarily a monolayer, and is free of extensive polymerization [1]. However, little was known concerning the initial structures formed in the surface-silylation reaction. One approach is to determine whether all the labile groups on the silicon atoms have reacted. This approach poses two requirements, protection of the initial monolayer from moisture and a highly sensitive surface analytical technique. Very sensitive inelastic-electron-tunneling spectroscopy (IETS), which gives information on the vibrational structure of organic monolayers on metal oxide surfaces [8] is particularly attractive. For this study, triethoxyvinylsilane was chosen because the triethoxy groups surviving the reaction can be distinguished easily from the stable vinyl group [9].

As seen in Fig. 1, good tunneling spectra (d^2i/dV^2 *versus V*) were obtained at 4.2 K for the vinylsilyl derivative A in the Al_2O_3-Pb sandwich junction. The IETS spectrum is relatively simple and compares well with the infrared (IR) spectrum for trichlorovinylsilane [10]. While not shown, the plot for the vinylsilyl structure reveals only a very small broad peak in the region near 3600 cm^{-1}, suggesting extensive removal of surface -OH groups [8]. Of particular interest are the bands at 1070, 2853, and 2944 cm^{-1}, which indicate the presence of -OCH_2CH_3 groups. When the aluminum surface is silylated with excess triethoxyvinylsilane but not rinsed, these bands become much stronger and other weaker bands appear, indicating that some ethoxy groups remain intact as Si-O-CH_2CH_3 and may be available for reaction with Lewis bases (see Scheme 1). It is unfortunate that the region between 800 and 1100 cm^{-1} is not well resolved because this region could provide some insight into the Si-O-Si and Si-O-Al bonding structure [11].

Scheme 1

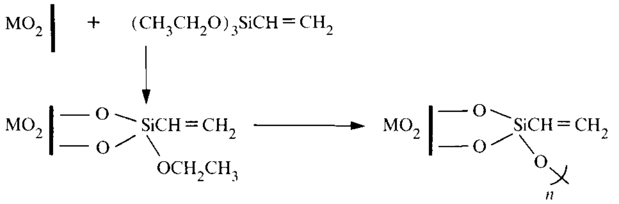

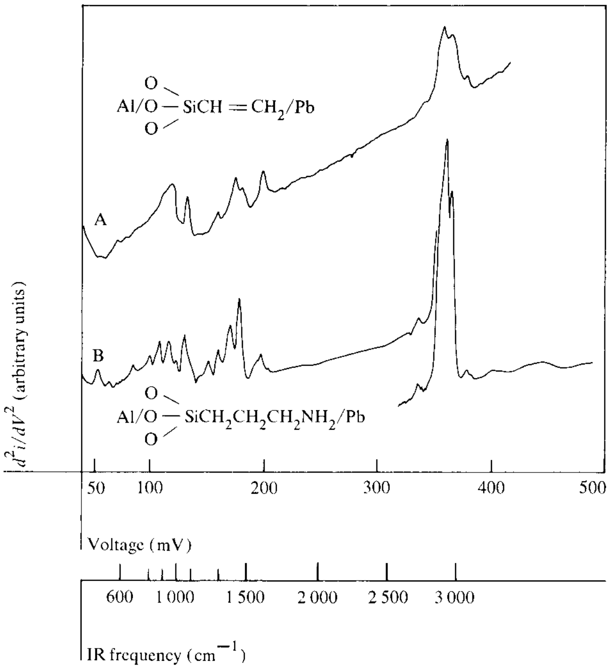

Figure 1 Tunneling spectra of (curve A) vinylsilyl and (curves B) 3-aminopropylsilyl derivatives at 4.2 K.

The major difference between the spectrum for the 3-aminopropylsilyl derivative (curve B) and the starting material, 3-aminopropyltriethoxysilane [10] is the position and the weakness of the N-H stretching bands at 3320 and 3250 cm^{-1} (displaced by about 80 cm^{-1}). This shift could be due to the presence of intermolecular hydrogen bonding [11]; however, it is dangerous to draw conclusions concerning the molecular structure of the 3-aminopropylsilyl insulating layer without clearly understanding the influence of the deposited lead contact.

Recall that the structure discussed here is the one initially formed in the reaction; this structure is preserved by the special conditions of the experiment. In practice, the remaining Si-OCH_2CH_3 groups react readily upon contact with moisture in the air, producing surface dimers and trimers with adjacent molecules.

Another important consideration in the characterization of these monolayers is the surface density Γ of the silyl derivative. Estimates of the surface densities have been obtained from electrochemical measurements, where a structure with known electrochemical behavior is attached to the terminal amino group of the aminoalkylsilyl derivative. The concentration is then estimated from the current-voltage plots. Values of Γ obtained in this manner must take into account the yields of the two surface reactions, silylation of the oxide surface and reac-

Error

An error occurred while processing this page. See the system log for more details.

ture Ib using a platinum button electrode shows peaks with E_{pa} values at 0.32 V (i_c/i_a = 1) and 1.00 V (irreversible) at 200 mV/s. Each peak is a one-electron-transfer process; in this case, the first reaction shows reversibility in the sweep range between 2 and 200 mV/s. This is seen in the data listed in Table 1, where the measurements were made with *iR* compensation.

$$\mathrm{Ic} \overset{-e^-}{\rightleftharpoons} \mathrm{Ic}^{+\cdot} \overset{-e^-}{\rightleftharpoons} \mathrm{Ic}^{++}$$

Of particular interest is the varying electrochemical behavior of anchored *vs* solubilized Structure II in solution.

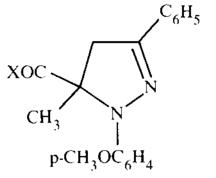

a : X = HO
b : X = CH$_3$O
c : X = SnO$_2$/Si3N2N

II

Surface-bonded IIc does not display the expected *i-V* curve for a reversible reaction. Instead, as seen in Fig. 2, the oxidation peak (E_{pa} = 0.43 V) shows only a small i_c signal in the return sweeps. After the first scan the oxidation peak is greatly reduced, and it is barely detectable in the third scan. From the first scan, Γ equals 7×10^{13} molecules/cm^2, uncorrected. The *i-V* curve for IIb using a platinum button electrode shows two peaks with E_{pa} values equal to 0.44 V (i_c/i_a = 1) and 1.09 (irreversible) at 200 mV/s. Again, each peak is a one-electron-transfer process. With *iR* compensation, the first reaction shows the same reversibility as Ib in the sweep range 2 to 200 mV/s. This is seen in Table 1. The same reversible behavior is observed with IIb using an untreated tin oxide electrode, SnO$_2$/Si3N2N, and acetylated SnO$_2$/Si3N2N.

While the monocyclic and tricyclic N-anisylpyrazoline derivatives in solution show the same high electrochemical reversibility under cyclic voltammetry conditions, the monocyclic radical cations show some decomposition (to produce the corresponding pyrazole) on a much longer time scale. The reaction occurs even when the pyrazoline is disubstituted in the 5 position, as in II, producing the 4,5-disubstituted pyrazole [13b, 15]. Thus, the pyrazole formation from the radical cation of IIc must be enhanced when it is bonded to the electrode; this results in an irreversible *i-V* curve. The formation of the pyrazole derivative from the pyrazoline derivative probably occurs as shown in Scheme 3. These results suggest that an array of

Scheme 3

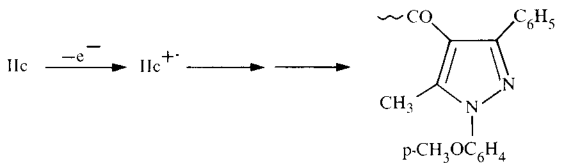

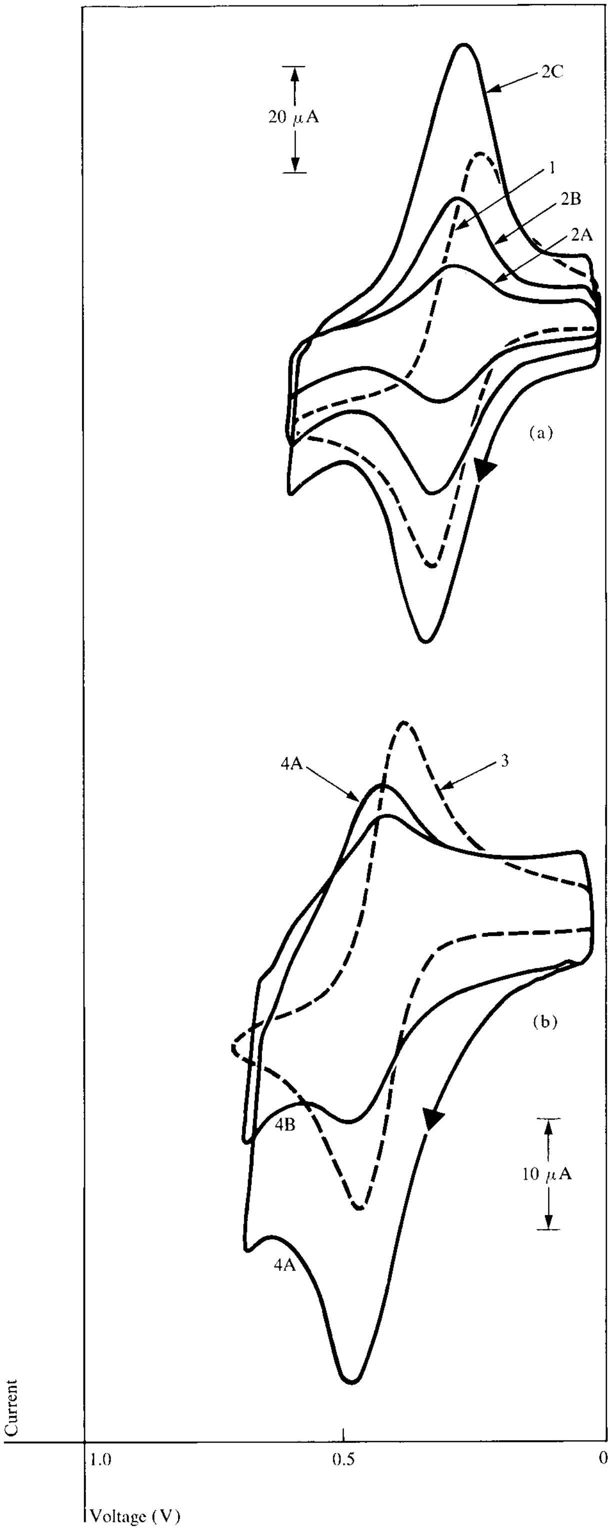

Figure 2 Cyclic voltammograms for (a) structure Ib in solution at 200 mV/s (dotted curve 1) and structure Ic surface-bonded (solid curves 2A-C) for scans at 50, 100, and 200 mV/s, respectively; and for (b) structure IIb in solution (dotted curve 3) and structure IIc surface-bonded (curves 4) at 200 mV/s. Curves 4A and 4B denote the first and second scans for IIc. The scales are indicated on each set of curves; all scans run in CH$_3$CN.

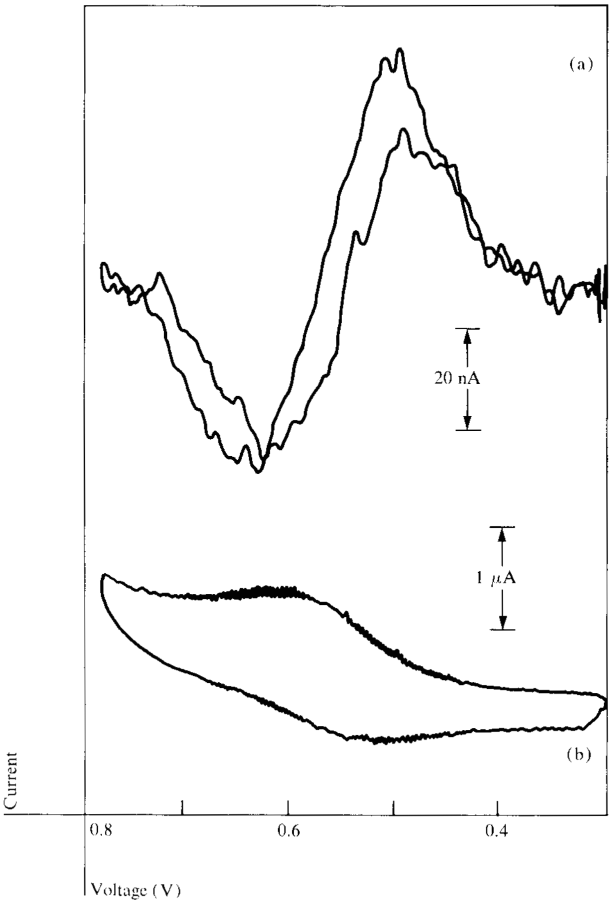

Figure 3 (a) Second-harmonic and (b) cyclic voltammograms measured in CH_3CN for the modified electrode SnO_2/Si3N2N (Ic). The cyclic voltammogram was run at a sweep rate of 40 mV/s.

radical ions bonded to the electrode surface is less stable than a similar group of radical ions that are free to diffuse into solution. This difference must result from variations in the solvating structure and the coulombic interactions.

The reduced stability of surface-bonded electroactive compounds has been observed with other systems. For example, dinitrobenzamide derivatives attached to RuO_2 [1d] or PtO_2 [1e] surfaces give electrochemical signals that decay within 10 to 20 minutes of voltage sweeping. In contrast, the solution spectra for these compounds show high electrochemical reversibility.

Although it is difficult to make a rigorous comparison it is useful to compare the observed stability of the covalently attached monolayer of electroactive structures with thicker polymer films that contain electroactive structures. The latter cases show a greater electrochemical reversibility; the redox reactions of incorporated structures such as ferrocene [16], nitrobenzene [17], and pyrazoline [18] can be cycled for over 24 hours. The principal difference between these two systems is that in the covalently attached monolayer the electroactive moiety lies within 1 nm (10 Å) of the electrode surface and the greatest potential gradient (10^6 V/cm [19]) is also in this region. This factor may contribute to the reduced stability of the electroactive structures. In the case of polymeric films, the redox reactions involve motion of the electroactive structures. Those structures that are close to the surface move in and out of a large potential-gradient region but do not necessarily reside in it. Thus, the stabilities of these structures should compare more closely with those of their dissolved counterparts.

It becomes apparent that analysis of attached species on modified electrode surfaces by cyclic voltammetry produces waveforms that are difficult to analyze quantitatively. The E_p values and concentrations of electroactive species can only be approximated because current levels resulting from surface coverage with attached material are significantly less than those attained by using normal concentrations of dissolved species and because the metal oxide surfaces currently being used inevitably produce high capacitive currents. As a result, it becomes difficult to discern small currents due to a Faraday process from large charging currents. This is especially true at higher sweep rates.

Second-harmonic ac voltammetry, a technique that strongly discriminates against double-layer charge currents in solution-soluble redox couples [20, 21], was used because of this. Anson [6a] has also used differential pulse voltammetry to minimize currents due to double-layer capacitive charging, and to detect pseudo-capacitive currents arising from absorbed reactants. Such a technique can also be applied in studying the kinetics of charge transfer at electrode surfaces.

Figure 3(a) shows the *i*-*V* plot of the second-harmonic ac voltammogram of the modified surface Ic. Unlike previously published results, ours show the recorded sweep of both the forward and reverse scans [22]. The curve is reasonably well-defined with a signal-to-noise ratio of about 10. Analytical considerations [23] based on Hubbard and Anson's treatment of the thin cell [24] show that the potential dependence of the second-harmonic waveform is identical to that obtained for solution spectra [20]. One can determine the thermodynamic halfwave potential from the cross-over potential. The peak-to-peak current excursion and the peak-to-peak voltage separation of the second-harmonic current are quantities that can be related to coverage and to the kinetics of electron transfer. The halfwave potential obtained by averaging the forward and reverse sweeps is +0.56 ± 0.01 V (*versus* NaCE). Measurements with a SnO_2/Si3N2N surface do not show any signals in this region. Assuming a one-electron transfer and an electrode area of 0.2 cm^2, the average peak-to-peak excursion of 49 nA gives a Γ equal to 1.3×10^{12} molecules/cm^2 at 25 Hz. The average peak-to-peak separation is 170 mV, much larger than the 67 mV predicted for a reversible electron transfer.

The cyclic voltammogram shown in Fig. 3(b) was measured simultaneously and provides a poorly defined peak ($\Gamma = 2 \times 10^{13}$ molecules/cm^2). There is a large discrepancy in the value of Γ obtained from these two measurements [$\Gamma(dc)/\Gamma(ac) = 15$], and the discrepancy is directly dependent on the ac frequency used. For example, for attached tetrathiafulvalene (Structure III), $\Gamma(dc)/\Gamma(ac) = 6$ at 25 Hz, but = 23 at 100 Hz.

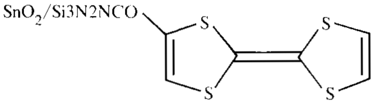

III

The solution spectra [Figs. 4(a), (b)] were obtained using a 0.2-cm^2 Pt-button electrode and a solution concentration of Structure IVa equal to 2×10^{-5} *M*. The second-harmonic voltammogram [Fig. 4(a)] had about the same signal-to-noise ratio as that for the modified electrode. The cyclic voltammogram [Fig. 4(b)] indicates a halfwave potential of +0.56 ± 0.01 V; $\Delta E_p \approx 70$ mV, indicating a reversible one-electron transfer. The bulk solution concentration was estimated to be 3×10^{-5} *M* from the second-harmonic voltammogram, and 4×10^{-5} *M* from the cyclic voltammogram. Agreement between the two methods is also seen with phenanthraquinone absorbed on carbon. Here, the two estimated concentrations are within five percent of each other and the agreement is independent of the ac frequency. Thus, the second-harmonic and cyclic voltammograms provide quite consistent results for cases involving dissolved and absorbed species, where the electron transfer rate is very fast.

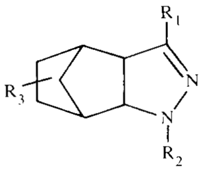

IV

a : $R_1 = C_6H_5$, $R_2 = p\text{-}CH_3OC_6H_4$, $R_3 = H$
b : $R_1 = R_2 = C_6H_5$, $R_3 = H$
c : $R_1 = R_2 = C_6H_5$, $R_3 = SnO_2$/Si3N2NCO

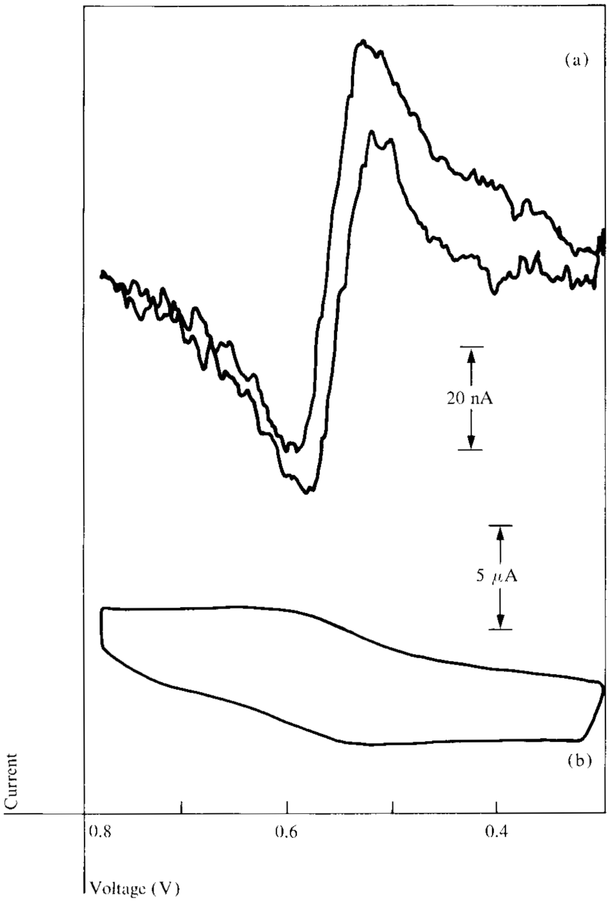

Figure 4 (a) Second-harmonic and (b) cyclic voltammograms measured in CH_3CN for a solution containing 2×10^{-5} *M* IVa. A Pt electrode is used for the second-harmonic voltammogram. A sweep rate of 200 mV/s is used for the cyclic voltammogram.

With covalently attached species, the reaction becomes electrochemically irreversible and only a fraction of the electroactive molecules exchange charge with the surface even at 25 Hz. Thus, the chemical environment of these structures must vary widely. Furthermore, the slow overall rate of charge transfer between these species and the surface may reflect the slow rate of interconversion of the electroactive moieties among the various environments.

Electrochemical behavior of surface attached radical ions

We now turn our attention to the chemical behavior of the surface-attached radical ions that are generated electrochemically (*i.e.*, the follow-up reactions of the intermediates), and we compare this behavior with that obtained for the solution counterparts.

The N-phenyltricyclopyrazoline derivative (Structure IVb) [14] was used because radical cations generated in

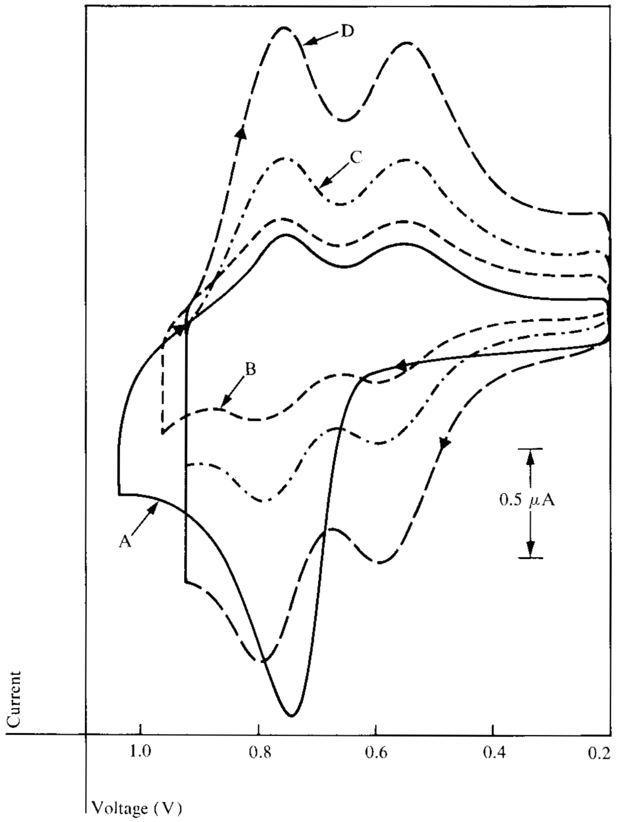

Figure 5 Cyclic voltammograms measured in CH_3CN containing 0.1 *M* Et_4NBF_4; NaCE reference electrode. Plots A (10 mV/s), B (10 mV/s), C (20 mV/s), and D (40 mV/s) are for the first (monomer IVc), and the second, third, and fourth scans (dimer V) with the modified surface, respectively.

Scheme 4

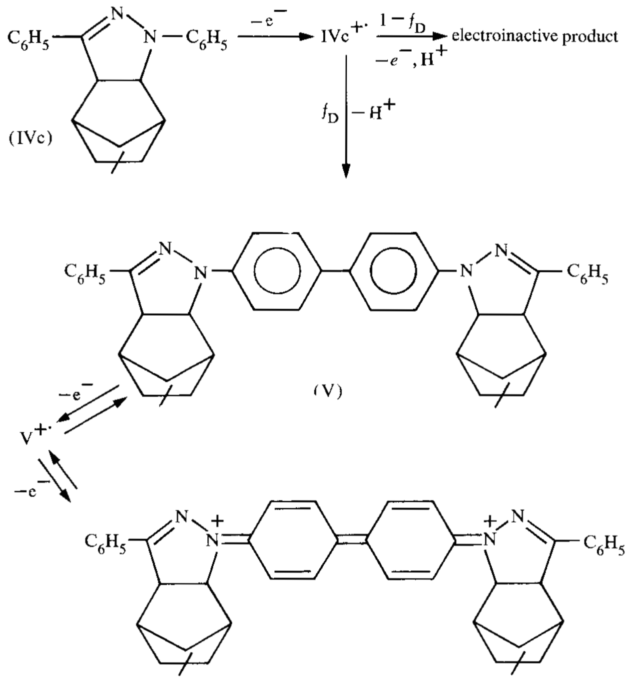

the electrochemical reaction are unstable and react rapidly to produce dimer V (see Scheme 4) in high yield [25, 26]. Furthermore, since the dimeric product is electroactive, the fate of the radical intermediate can be analyzed electrochemically. Shown in Fig. 5 are the cyclic voltammograms for a modified SnO_2 surface containing the attached N-phenyltricyclopyrazoline derivative IVc [13]. No *iR* compensation was used in these measurements. In the first scan, the anodic sweep produces a single peak corresponding to an irreversible reaction while two small peaks appear in the reverse sweep. In the second scan, the initial signal at +0.75 V is not present; instead, signals for two reversible couples appear at +0.57 V and +0.79 V. The peak-to-peak separation, $E_{pa} - E_{pc}$, for each couple is not zero as would be expected for a reversible, attached species. Instead, in each case it is 40 mV and this separation does not vary with sweep rate between 10 and 80 mV/s. On the other hand, the peak heights scale linearly with sweep rate as would be expected for an attached species. These results are consistent with a bonded quasi-reversible redox species.

The most interesting observation is the marked difference between the first and all subsequent scans of the cyclic voltammograms made on the same modified electrode surface. The first scan agrees with that obtained using a clean platinum or tin oxide surface and the dissolved N-phenylpyrazoline derivative (IVb) [25]. A spectroscopic study of this electrochemical reaction using dissolved species [26] reveals that the initially formed N-phenylpyrazoline radical cation reacts rapidly to produce 95% dimer V and 5% pyrazole VI. The dimeric product is further oxidized in two one-electron reactions with potential values similar to that for the original N-phenylpyrazoline derivative. Thus, during the first scan (Fig. 5, plot A) the dication of the dimeric product is generated. The reverse sweep then displays peaks for each of the reduction reactions to regenerate the neutral dimeric product. The second scan (plot B) shows the waves for the electrochemically reversible reactions of dimeric product at +0.57 V and at +0.77 V to produce the radical cation and dication species, respectively. These reactions are summarized in Scheme 4.

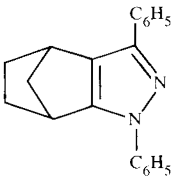

VI

Considering that the signal observed in the first scan (A) involves the transfer of two electrons per molecule

[26], the surface concentration of N-pyrazoline derivative is estimated from the area under the peak (uncorrected) to be 8×10^{13} molecules/cm^2. The amount of dimer produced from the initially formed radical cation is estimated from the second scan, and is found to vary with the sweep rate of the first scan. The fraction of dimeric product formed, f_D, is 0.06, 0.14, 0.28, 0.42, and 0.52 when the sweep rate for the first scan is 200, 80, 20, 10, and 2 mV/s, respectively. These values were obtained by comparing the relative areas under the signals in the i-V plot using $n = 2$ for the first scan and $n = 1$ for each peak in the second scan. (A 100% yield of dimer corresponds to an f_D equal to 0.50.)

The results are clearly different from those observed with dissolved species where the main reaction is radical combination to produce dimer. They imply that with surface-attached species, molecular motion is a limiting process. The variation of F_D with sweep rate reflects variation in the dimer forming process, which has a second-order kinetic dependence with respect to the radical cation and, therefore, depends on the molecular motion of the intermediate. The variation probably does not reflect changes in the radical cation aromatization process since this reaction is first-order with respect to the radical cation and is considerably less sensitive to its molecular motion.

With sufficiently slow sweeps, the molecular reorganization will permit the pyrazoline derivative to approach the SnO_2 surface in a situation analogous to that for the dissolved species, *i.e.*, where the appropriate conformation for charge transfer and dimerization of the pyrazoline structures is attained (f_D). With faster sweeps, the reorganization process is limited; thus the charge transfer must occur with the pyrazoline derivatives in different environments, some being away from the SnO_2 surface. Thus, the radical intermediates are generated in molecular orientations that are not appropriate for dimerization, and in these cases aromatization becomes important ($1 - f_D$). A preliminary treatment of these data indicates that the encounter rate for two attached pyrazoline moieties is about 10^4 more difficult than for dissolved species [23].

It is interesting to compare these results with those obtained with a TiO_2-attached 2-(α-pyridyl)ethylsilane derivative that was subsequently treated with CH_3I to produce the N-methylated derivative in 50% yield. This material can be regenerated in 30% yield when it is reduced to the dimer and then reoxidized; on a SnO_2 electrode, however, the same compound does not produce a reoxidizable dimer [1c].

Monolayer-electroactive solute interactions

We now present the results of measurements probing the influence of surface molecules on the electrochemical reactions of compounds in solution. A comparison is made of the influence of surface-attached alkylsilyl derivatives on electrochemical reactions when the electroactive species are attached and when they are in solution.

The presence of electroinactive molecular monolayers on electrode surfaces has been shown to influence electrochemical reactions. For example, the presence of olefinic compounds on a platinum surface slows reactions of platinum complexes in aqueous solutions [27]. Modified carbon [2] and metal oxide [2c] surfaces to which optically active derivatives are covalently attached have been shown to affect the relative rates for the formation of enantiomeric products. The cyclic voltammograms for several reversible electrochemical reactions using chemically modified SnO_2 [1a] and PtO_2 [1c] surfaces show unusually large $E_{pa} - E_{pc}$ separations compared with the unmodified surfaces, suggesting that the reactions become irreversible in the presence of surface molecules. Since this evidence is only qualitative, it is important to determine quantitatively the influence of electrode surface molecules on the charge-transfer rate.

For this particular study, we investigated the two reversible couples, phenothiazine(Structure VII)-phenothiazine radical cation, and benzoquinone(VIII)-benzoquinone radical anion in solution. We applied Nicholson's treatment [28] for estimating the heterogeneous rate constant k_s for simple, quasi-reversible electrochemical reactions,

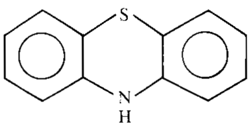
VII

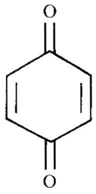
VIII

$$O + ne^- \overset{k_s}{\rightleftharpoons} R.$$

These two reactions were selected because the first electron-transfer step is electrochemically reversible (Table 1) and separable from any subsequent reactions. All electrochemical measurements were performed using 80–90% iR compensation.

As can be seen in Table 2, the first oxidation reaction displays complete reversibility on both platinum and SnO_2 surfaces. In contrast, the results with chemically modified electrode surfaces vary with the alkyl group on

Table 2 Cyclic voltammetric data for the oxidation of phenothiazine in CH_3CN; solutions contain 1×10^{-3} *M* phenothiazine plus 0.1 *M* Et_4NBF_4.

Electrode	*Sweep rate* (mV/s)	E_{pa}* (mV)	E_{pc}* (mV)	ΔE_p (mV)	ψ†	k_s (10^{-4} cm/s)
Platinum	10 to 100	650	590	60	—	—
SnO_2	10 to 100	650	590	60	—	—
SnO_2/SiC_2H_3	10 to 100	660	600	60	—	—
$SnO_2/Si(CH_2)_3NH_2$	10	728	630	98	0.606	32.4
	20	735	622	113	0.416	
	30	740	619	121	0.352	
	40	745	615	130	0.300	
	50	750	610	140	0.256	
	100	762	600	162	0.182	
SnO_2/Si3N2N	10	700	600	100	0.590	27.4
	20	710	590	120	0.350	
	30	715	580	135	0.270	
	40	725	575	150	0.220	
	50	730	570	160	0.195	
	100	765	550	215	0.095	
SnO_2/Si3N2NHCOC$_2$H$_5$	10	720	590	130	0.295	17.2
	20	730	580	150	0.215	
	30	750	570	180	0.145	
	40	760	560	200	0.115	
	50	770	550	220	0.090	
	100	825	525	300	—	

*E_p vs NaCE.
†Reference [28].

Table 3 Cyclic voltammetric data for the reduction of benzoquinone; solutions contain 1×10^{-3} *M* benzoquinone plus 0.1 *M* Et_4NBF_4; E_p are *versus* NaCE.

Electrode	*Sweep rate* (mV/s)	E_{pc} (mV)	E_{pa} (mV)	ΔE_p (mV)	ψ*	k_s (10^{-4} cm/s)
Platinum	10 to 100	−540	−480	60	—	—
SnO_2	10 to 100	−480	−420	60	—	—
SnO_2/SiC_2H_3	10	−490	−395	95	0.67	31.0
	20	−500	−390	110	0.45	
	30	−502	−385	117	0.38	
	40	−505	−380	126	0.33	
	50	−510	−375	135	0.27	
	100	−530	−350	180	0.15	
$SnO_2/Si(CH_2)_3NH_2$	10	−570	−340	230	—	10.4
	20	−580	−320	260	—	
	30	−595	−295	300	—	
	40	−610	−285	325	—	
	50	−620	−270	350	—	
SnO_2/Si3N2N	10	−710	−370	340	—	10.1
	30	−740	−350	390	—	
	50	−750	−270	470	—	
	100	−780	−200	580	—	
SnO_2/Si3N2NHCOC$_2$H$_5$	10	−630	−380	250	—	9.68
	20	−640	−350	290	—	
	30	−660	−340	320	—	
	40	−680	−320	360	—	
	50	−690	−310	380	—	
	100	−750	−260	490	—	

*Reference [28].

the surface-attached silyl derivative, ≡SiR. When the alkyl group is a vinyl group, the results resemble those with platinum, the only difference being a slight variation in E_{pa}. On the other hand, with the 3-aminopropyl and the 3-(2-aminoethylamino)propyl groups, the electrochemical reaction becomes irreversible. With the use of Table 1 in

Reference [28], Nicholson's ψ values can be obtained for the corresponding ΔE_p values measured at various sweep rates ν, and the k_s values were determined from the $\psi - \nu^{-1/2}$ plots. For the present reaction at 25°C, ψ is equal to $25.5 k_s \nu^{-1/2}$.

The ΔE_p values measured for some of the other modified surfaces lie outside the range of ψ values provided by Nicholson and make the method inapplicable. Nicholson's treatment was extended to obtain relative k_s values for a given reaction under identical conditions where only the nature of the working electrode is varied. Since the relation between $n\Delta E_p$ and $1/\psi$ is nearly linear, this extension can be made if one assumes a small continuing curvature. The slope S of the curve obtained by plotting $n\Delta E_{p(SnO_2/SiR')}$ measured with one electrode against $n\Delta E_{p(SnO_2/SiR)}$ measured with another electrode for the same values of $\nu^{1/2}$ is given by Eq. (1). The measurements with the 3-(2-aminoethyl)propylsilyl derivatized surface were selected for the relationship

$$\frac{d|n\Delta E_{p(SnO_2/SiR')}|}{d|n\Delta E_{p(SnO_2/SiR)}|} = S\left[\frac{k_{s(SnO_2/SiR)}}{k_{s(SnO_2/SiR')}}\right] \qquad (1)$$

in Eq. (1). The $\psi - \nu^{-1/2}$ plot for this reaction is seen in Fig. 6.

The use of this relationship is seen in Fig. 7, where the plot of ΔE_p values measured with the surface-attached 3-(2-propionylaminoethylamino)propylsilyl group *versus* ΔE_p values measured with the surface-attached 3-(2-aminoethylamino)propylsilyl group provides a straight line with slope S of 1.5 ± 0.1 within the sweep range considered. This slope yields a k_s value of 18.5×10^{-4} cm/s for the reaction of the electrode containing the surface-attached amide group, which is essentially the same as that obtained directly from the Nicholson treatment (17.2×10^{-4} cm/s).

For the benzoquinone reduction reaction ψ is equal to $23.6 k_s \nu^{-1/2}$. As in the previous case, this reaction appears completely reversible on platinum and SnO_2 surfaces. The reaction is, however, sensitive to all surface modifications, as seen in Table 3. Equation (1) and the k_s value for the attached vinylsilyl group were used to determine k_s values for all the other modified surfaces. A linear relationship was obtained in every case, the fit being ≈4%.

The presence of small molecules covalently attached to the electrode surface can have a significant effect on the rates of electrochemical reactions. When surface molecules are aliphatic derivatives the rates are reduced. This rate reduction must be due primarily to steric effects. These results parallel studies by Lane and Hubbard of absorbed olefinic compounds on platinum surfaces [27].

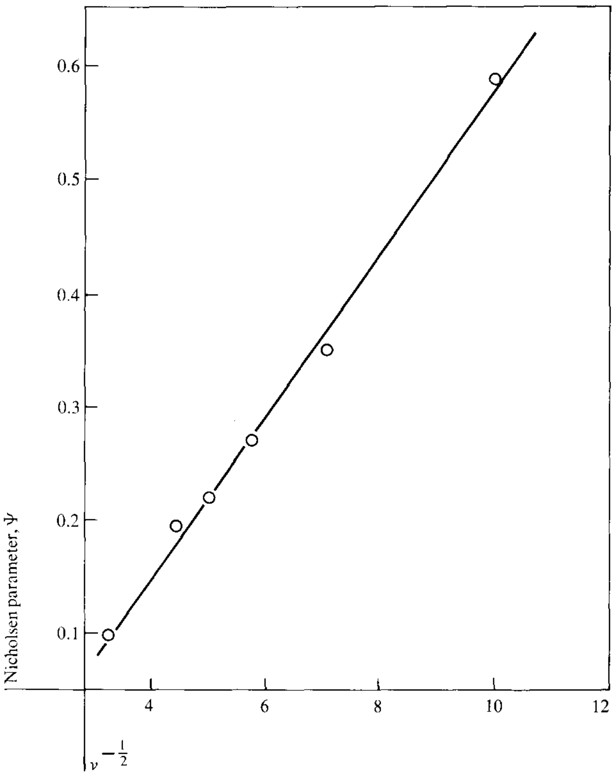

Figure 6 Plot of ψ *versus* $\nu^{-1/2}$ for the reaction of phenothiazine on a SnO_2/Si3N2N surface. The rate constant k_s is 27.4×10^{-4} cm/s; CH_3CN solution *versus* NaCE reference electrode.

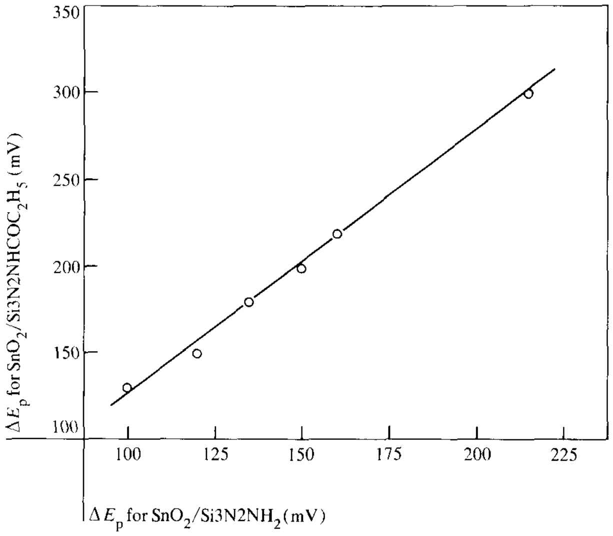

Figure 7 Plot of ΔE_p changes on the two surfaces for the reaction of phenothiazine as a function of sweep rate; NaCE reference electrode, CH_3CN solution, and slope $S = 1.5 \pm 0.1$.

The influence of these molecules on SnO_2 is similar for both electrochemical reactions. The major difference is in the case of the phenothiazine-phenothiazine radical-cat-

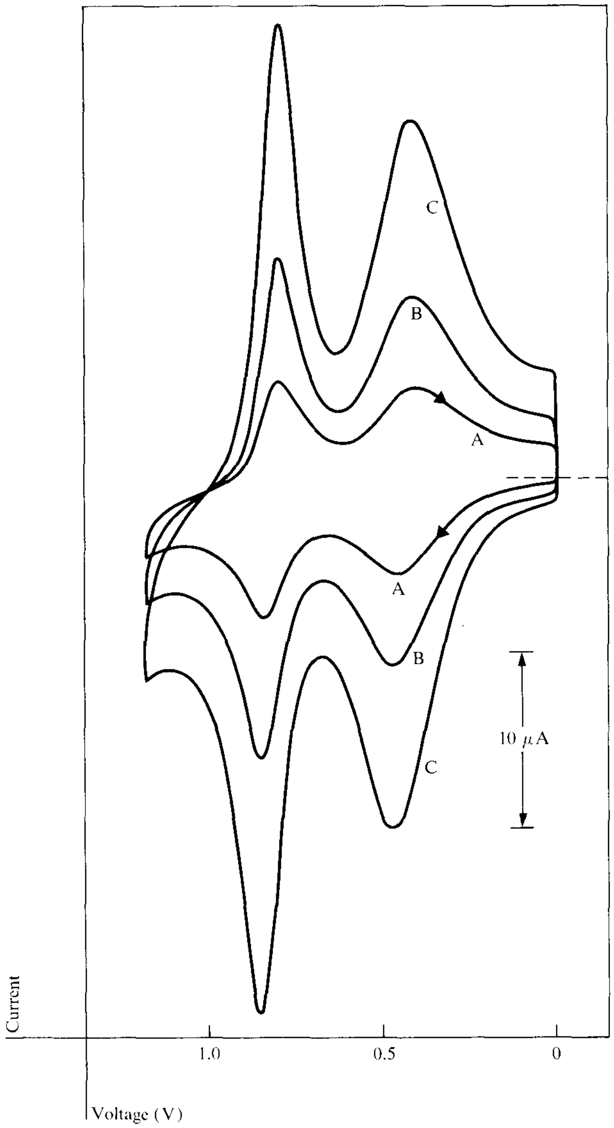

Figure 8 Cyclic voltammogram for attached TTF in CH_3CN containing 0.1 *M* Et_4NBF_4 with approximately 70% *iR* compensation; modified SnO_2/Si3N2NHCOTTF surface (0.2 cm^2) *versus* NaCE. Curves A, B, and C are at sweep rates of 50, 100, and 200 mV/s, respectively.

ion reaction, where the reaction is not influenced by the presence of the surface vinylsilyl group. In such cases, the reactions display high reversibility, as was the case with platinum and tin oxide surfaces. However, the presence of these surface groups reduces the reaction rate by a factor of about 340 (by using a reference k_s value of 1 cm/s for the reaction on a platinum surface [29]).

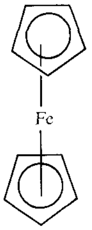

IX

The influence of steric effects was also studied by looking at the oxidation of ferrocene (Structure IX). Ferrocene is structurally different from phenothiazine and benzoquinone in that it is more spherical. On platinum the reaction is reversible, as seen in Table 1. However, the reaction shows irreversibility on the SnO_2 surface and is strongly influenced by any surface modification. In these cases, the peaks were too broad and separated to continue any further. The marked difference in behavior between this reaction and those discussed previously emphasizes the complexity of the electrode process and could be explained by considering that the electroactive species must penetrate the surface molecules and come in close contact with the electrode surface in order for electron transfer to occur. This is not unreasonable since surface coverages in these preparations are less than a closely packed monolayer.

Very similar results were obtained when modified PtO_2 surfaces (rather than SnO_2) containing covalently attached monolayers of the various alkylsilyl derivatives were studied. The differences observed were with the larger alkyl groups that produce a more pronounced effect on the reaction [30].

Several reports have recently appeared in the literature describing the use of electrodes containing surface-bonded optically active compounds to study reactions that produce an enantiomeric product mixture [2]. In contrast to the present results, the surface molecules in these cases have a small influence; the enantiomeric excess found in the products is 2-10%. These reactions are multistep, and although the surface molecules may have a large effect on the charge transfer rate, they have only a small effect in the product forming step of the reaction, where the stereochemistry of the molecule is determined. This minimal influence of the surface molecules on the electrochemistry of the products implies that the reaction intermediates must diffuse away from the surface before forming the product.

It is interesting to contrast these results using covalently attached monolayers with those using thin polymer films (the other surface modification technique of current interest). Since this comparison can best be made using reasonably well defined polymers, plasma polymerized tetrafluoroethylene films were selected for this study.

These films are prepared such that they do not swell, are both rigid and highly cross-linked, adhere strongly to metal surfaces and do not lift off, are pinhole free, and the molecular structure contains cavities equivalent to eight member rings [31]. The electrochemical oxidation of ferrocene in acetonitrile solution using a platinum electrode coated with 2.5 nm of polymerized tetrafluoroethylene film is quasi-reversible. No variation is observed in the redox potential; thus the chemical environment around the ferrocene at the electrode surface must be similar to that with a clean surface. The k_s value obtained using Nicholson's treatment [28] is 6×10^{-3} cm/s. Therefore, this 2.5-nm polymer film has less retarding effect on the solution reaction than the ≈0.8-nm covalently attached film. With much thicker films, 20–60 nm, the redox reaction of ferrocene still occurs at the platinum-polymer interface; however, the reaction is limited by the diffusion of ferrocene through the film. In this case, the diffusion rate through the film is a factor of 10^5 slower than through the acetonitrile solution. These results indicate that dissolved species can penetrate polymer films on electrode surfaces. The penetration occurs even with the rigidly crosslinked polymer and may be more effective with other polymers that swell with solvent.

The final topic of this presentation involves the redox reaction of a species in solution on a modified electrode surface where the covalently attached monolayer contains an electroactive center. The involvement of the attached electroactive species as a mediator in the overall reaction provides a potential route to designing molecule-specific electrodes [3a, 4]. This would be accomplished by making use of specific mediator-electroactive molecule interactions that enhance the electron transfer rate. To demonstrate the feasibility of using an electron mediator model, ferrocene in acetonitrile solution was oxidized on a modified surface where the covalently attached monolayer contains a tetrathiafulvalene (TTF) structure. Figure 8 shows the cyclic voltammogram for TTF on the surface as in Structure III [32]. This reaction shows good electrochemical reversibility for each of the two one-electron oxidation reactions [1h]. Figure 9 shows the cyclic voltammogram for the surface III in the potential region involving the first oxidation reaction. When the solution contains 10^{-3} *M* ferrocene, broad deformed oxidation and reduction peaks are seen. This system is not stable, however, and the peaks diminish gradually until after the twelfth scan no further change occurs. This instability probably reflects decomposition of the tetrathiafulvalene structure rather than the entire monolayer. This conclusion is based on the fact that the twelfth scan resembles that for a modified surface with a covalently attached electroinactive monolayer rather than that for a clean SnO_2 surface (Fig. 10). While these results are preliminary, they do show that the electroactive monolayer is involved in the overall reaction and probably behaves as an electron-transfer mediator.

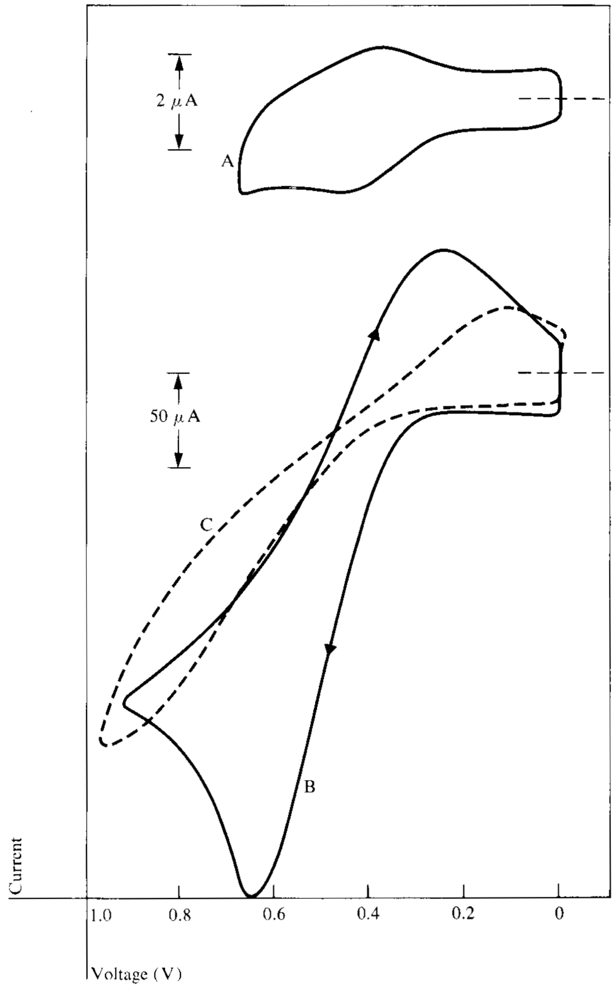

Figure 9 Cyclic voltammograms measured using a modified surface SnO_2/Si3N2NHCOTTF *versus* NaCE. (Curve A) 0.1 *M* Et_4NBF_4 in CH_3CN, 50 mV/s; (curve B) 0.1 *M* Et_4NBF_4 plus 10^{-3} *M* ferrocene in CH_3CN, first scan at 50 mV/s; (curve C) same as curve B but after twelfth scan.

Conclusions

In summary, the brief study presented here permits us to make certain statements. In regard to the molecular structure, the initially formed structures of the alkylsilyl derivatives on metal oxide surfaces contain some unreacted labile alkoxide groups. This suggests that the final product may have some polymeric nature. When the electroactive species are attached to the surface via linear alkylsilyl derivatives, they appear to exist in various chemically different environments. Interconversion of the electroactive moieties among the various environments is slow and depends on the folding behavior of the linear alkylsilyl de-

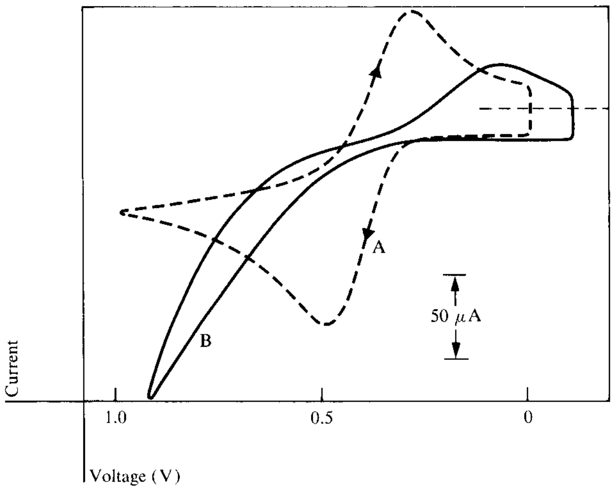

Figure 10 Cyclic voltammograms of 10^{-3} *M* ferrocene measured on SnO_2 (curve A) and on SnO_2/Si3N2NHCOCH$_3$ (curve B) against NaCE in CH_3CN containing 0.1 *M* Et_4NBF_4 at 50 mV/s with approximately 80 percent *iR* compensation.

rivatives. The net effect is that redox reactions become electrochemically quasi-reversible. This behavior can influence the rate of charge transfer as well as the chemistry of the resulting radical cations, where those cations attached to the surface via flexible alkyl chains have more restricted mobility than those dissolved in solution. Also, the array of radical ions produced under these conditions must be less stable than when they are free to diffuse into the solution. Finally, when the electroactive compound is in solution, the presence of alkylsilyl derivatives on the surface will again influence the electrochemical reaction where the movement of electroactive species in and out of the surface environment is retarded. However, when the alkylsilyl monolayer contains an electroactive center, electron-transfer to an electroactive species in solution is facilitated where the attached electroactive center can act as a mediator.

Experimental details

- *Preparation of silylated surfaces*

The modified surfaces were conveniently prepared by treating the cleaned surface with an anhydrous toluene solution containing about 1% of the alkylsilyl derivative for 10 minutes at room temperature. The surface was then washed with several portions of fresh toluene. The platinum surfaces were oxidized electrolytically in 1 *M* H_2SO_4, as previously described [1e] and silylated as above.

- *IETS measurements*

The metal/insulator/metal sandwiches of 1 mm cross section were prepared on clean 10 × 15 mm glass slides. The slide with a freshly prepared aluminum oxide strip (1 mm wide) was treated with 1% volume fraction triethoxyvinylsilane in benzene in the usual manner. A 1-mm-wide strip of lead was subsequently evaporated on the dried surface, producing a junction with resistances in the range 50-5000 Ω/cm^2. The junction was next mounted for cooling to 4.2 K and the measurements were performed as previously described [8].

- *Synthesis of 2-pyrazoline derivatives*

Synthesis of these compounds makes use of the addition reaction of the diarylnitrile imine to the appropriate olefin [14]. For example, Structure I was prepared by the addition of diarylnitrile imine to exo-2-carbomethoxy-5-norbornene to produce Ib, which was then saponified in aqueous methanol to yield the carboxylic acid derivative Ia. This preparation produces a 1:1 mixture of the two possible exo-adducts [13b]. The monocyclic derivatives II were prepared as above using methyl methacrylate in the nitrile imine addition reaction [13b].

- *Electrochemical measurements*

The instrumentation used for dc voltammetry and chronocoulometry measurements were designed and fabricated in these laboratories [33]. For the second-harmonic ac voltammetry study, a small 25-Hz sinusoid (7.1-mV root mean square) from a Hewlett-Packard 3310A function generator was summed with a triangular ramp voltage. This signal was potentiostatically applied to the cell. A voltage proportional to the cell current was passed through a 25-Hz notch filter and then to a type A preamplifier of a Princeton Applied Research HR-8 lock-in detector. The second-harmonic reference was generated from the square wave synchronous output from the HP3310A generator. The scans were recorded on a Hewlett-Packard 7046A dual pen recorder.

All the electrochemical measurements were carried out in acetonitrile containing 0.1 *M* tetraethylammonium tetrafluoroborate. The solvents and the various compounds used were purified as previously described [13]. For these measurements, 10 mm × 30 mm plates of commercially available antimony-doped SnO_2 on glass were silylated.

Acknowledgments

The authors wish to acknowledge R. Hernandez and R. Galwey for their technical support, M. Genies, U. Hetzler, A. Dilks, D. Green, C. Snyder, F. Orozco, and J. Paredon for their collaboration, and H. Seki for his general support in the initial development of this project. This paper was presented in part at the Symposium on Silylated Surfaces, Midland, Michigan, May 1-3, 1978.

References

1. (a) P. R. Moses, L. Wier, and R. W. Murray, *Anal. Chem.* **47,** 1882 (1975); (b) C. M. Elliot and R. W. Murray, *Anal. Chem.* **48,** 1247 (1976); (c) P. R. Moses and R. W. Murray, *J. Amer. Chem. Soc.* **98,** 7435 (1976); (d) P. R. Moses and R. W. Murray, *J. Electroanal. Chem.* **77,** 393 (1977); (e) J. R. Lenhard and R. W. Murray, *J. Electroanal. Chem.* **78,** 195 (1977); (f) D. F. Untereker, J. C. Lennox, L. M. Wier, P. R. Moses, and R. W. Murray, *J. Electroanal. Chem.* **81,** 309 (1977); (g) J. R. Lenhard, R. Rocklin, H. Abruna, K. Willman, K. Kuo, R. Nowak, and R. W. Murray, *J. Amer. Chem. Soc.* **100,** 5213 (1978), and references therein; (h) R. W. Murray, Presentation at the Symposium on Silylated Surfaces, Midland, MI, May 1-3, 1978.
2. (a) B. F. Watkins, J. R. Behling, E. Kariv, and L. L. Miller, *J. Amer. Chem. Soc.* **97,** 3549 (1975); (b) B. E. Firth, L. L. Miller, M. Mitani, T. Rogers, J. Lennox, and R. W. Murray, *J. Amer. Chem. Soc.* **98,** 8271 (1976); (c) B. E. Firth and L. L. Miller, *J. Amer. Chem. Soc.* **98,** 8272 (1976).
3. (a) J. F. Evans and T. Kuwana, *J. Electroanal. Chem.* **80,** 409 (1977); (b) *Anal. Chem.* **49,** 1634 (1977).
4. (a) R. J. Burt, G. J. Leigh, and C. J. Pickett, *J. Chem. Soc., Chem. Commun.*, 940 (1976); (b) J. L. Leigh and C. J. Pickett, *J. Chem. Soc. A*, 1797 (1977).
5. (a) M. S. Wrighton *et al.*, *J. Electroanal. Chem.* **87,** 429 (1978); (b) M. S. Wrighton *et al.*, *J. Amer. Chem. Soc.* **100,** 1602 (1978); (c) J. M. Bolts and M. S. Wrighton, *J. Amer. Chem. Soc.* **100,** 5257 (1978), and references therein.
6. (a) A. P. Brown, C. Koval, and F. C. Anson, *J. Electroanal. Chem.* **72,** 379 (1976); (b) A. P. Brown and F. C. Anson, *J. Electroanal. Chem.* **83,** 203 (1977); (c) N. Oyama and F. C. Anson, *J. Electroanal. Chem.* **88,** 289 (1978); (d) N. Oyama, A. P. Brown, and F. C. Anson, *J. Electroanal. Chem.* **87,** 435 (1978).
7. I. Haller, *J. Amer. Chem. Soc.* **100,** 8050 (1978).
8. M. G. Simonsen, R. V. Coleman, and P. K. Hansma, *J. Chem. Phys.* **61,** 3789 (1974).
9. A. F. Diaz, U. Hetzler, and E. Kay, *J. Amer. Chem. Soc.* **99,** 6780 (1977).
10. The Aldrich Library of Infrared Spectra, Charles J. Pouchert, Aldrich Chemical Co., Inc., New York.
11. L. J. Bellamy, *The Infrared Spectra of Complex Molecules*, John Wiley & Sons, Inc., New York, 1964.
12. C. Snyder and A. Diaz, presented at Pacific Conference on Chemistry and Spectroscopy, San Francisco, September 27-29, 1978.
13. (a) A. Diaz, *J. Amer. Chem. Soc.* **99,** 5383 (1977); (b) A. Diaz, *J. Org. Chem.* **42,** 3949 (1977).
14. R. Huisgen, M. Seidel, G. Wallbillch, and H. Knupfer, *Tetrahedron* **17,** 3 (1962).
15. F. Pragst and C. Boch, *Electroanal. Chem.* **61,** 47 (1975).
16. (a) A. Merz and A. J. Bard, *J. Amer. Chem. Soc.* **100,** 3222 (1978); (b) K. Itaya and A. J. Bard, University of Texas, Austin, 1978, private communication.
17. L. L. Miller and M. R. Mark, *J. Amer. Chem. Soc.* **100,** 3223 (1978).
18. F. Kaufman and E. Engler, submitted to *J. Amer. Chem. Soc.*
19. J. O'M. Bockris and A. K. N. Reddy, *Modern Electrochemistry*, Plenum Publishing Co., New York, 1970.
20. A. M. Bond, R. J. O'Halloran, I. Ruzic, and D. E. Smith, *Anal. Chem.* **48,** 872 (1976).
21. M. R. Wasielewski and R. Breslow, *J. Amer. Chem. Soc.* **98,** 4222 (1976).
22. A. F. Diaz and K. K. Kanazawa, *J. Electroanal. Chem.* **86,** 441 (1978).
23. K. K. Kanazawa (IBM Research Division, San Jose, CA), unpublished results.
24. (a) A. T. Hubbard and F. C. Anson, *Electroanalytical Chemistry*, vol. 4, A. J. Bard, ed., Marcel Dekker, New York, 1970; (b) A. P. Brown and F. C. Anson, *Anal. Chem.* **49,** 1589 (1977).
25. N. A. Evans, D. E. Rivett, and J. F. K. Wilshire, *Aust. J. Chem.* **77,** 2267 (1974).
26. M. Genies and A. Diaz, *J. Electroanal. Chem.*, in press (1979).
27. R. F. Lane and A. T. Hubbard, *J. Phys. Chem.* **77,** 1411 (1973).
28. R. S. Nicholson, *Anal. Chem.* **37,** 1351 (1965).
29. M. E. Peover, *Reactions of Molecules on Electrodes*, N. S. Husk, ed., Wiley-Interscience, New York, 1971, Chapter 5, p. 259.
30. J. Paredon (Laboratorio de Investigaciones Eléctricas, Cuernavaca, Morelos, Mexico), unpublished results, 1978.
31. A. F. Diaz, A. Dilks, K. K. Kanazawa, and E. Kay, *J. Electroanal. Chem.*, in press, 1979.
32. D. Green (IBM Research Division, Yorktown Heights, NY) and A. Diaz (IBM Research Division, San Jose, CA), unpublished results, 1978.
33. K. K. Kanazawa and R. Galwey, *J. Electrochem. Soc.* **124,** 1385 (1977).

Received November 7, 1978; revised December 11, 1978

The authors are located at the IBM Research Division laboratory, 5600 Cottle Road, San Jose, California 95193.